DYNAMIC EARTH PRESSURE ON EMBEDDED STRUCTURES

W. Sarfeld (I)
S.A. Savidis (II)
H. Klapperich (I)
Presenting Author: S.A. Savidis

SUMMARY

Extensive large scale experimental investigations on a shaking table were carried out in order to determine the dynamic earth pressures on symmetrical and non-symmetrical embedded structures caused by seismic excitation. The dynamic earth pressure is split in two parts: an elastic oscillating part and a plastic part - the sum of both in addition to the static initial stresses leads to the total dynamic earth pressure. Numerical investigations with FE calculations were carried out for verification of experimental data of the elastic part and to study dynamic soil structure interaction, especially kinematic interaction.

INTRODUCTION

Investigations of earthquake effects on structures have to consider the dynamic earth pressure problem. Determination of its characteristics, amount and distribution is necessary using it for input data in a dynamic analysis regarding a safety and economic design. For practical purposes, dynamic earth pressures are often calculated by the quasi-static method developed by MONONOBE/OKABE (1) for design of retaining structures (plastic solution). Considering basement walls during earthquakes there is no certain movement of the wall to produce a state of plastic equilibrium behind the wall. In addition, occasional failures of structures designed by that method show that it's not as conservative as is often supposed. Basic papers regarding the dynamic earth pressure problem were presented by SEED/WHITMAN (2), NAZARIAN/HADJIAN (3) and WHITMAN (4). KAUSEL et al (5) consider the seismically induced sliding of massive structures with special emphasis on dynamic structure characteristics and interaction of soil-structure. To clarify the physical phenomenon of dynamic earth pressure in terms of its static and dynamic components as well as its influence on the response of structures extensive large scale experimental investigations on a shaking table have been carried out. Beside verification of experimental results like distributions of pressures and response of structures with Finite Element calculations, interaction effects are illustrated.

(I) research assistent, Technical Univ. Berlin, FRG
(II) Professor, Technical Univ. Berlin, FRG
Demokritos Univ. Thrazien, Greece

EXPERIMENTAL INVESTIGATIONS

Tests have been carried out at the test area of the "Grundbau-Institut", Technical University Berlin using a large shaking table (8,0x2,0 m) which is moved horizontally by an 100 kN actuator of a hydraulic pulse plant. To study the influence of different parameters a harmonic base excitation was chosen. Fig. 1 shows the test equipment for an unsymmetrically embedded model structure. Fig. 2 presents the investigated models, allowing interaction between structure and surrounding soil. Recorded test data are stresses, displacements and accelerations - the former are measured in the interface structure - soil by piezoresistive stress transducers and the latter are registrated from the model structure as well as from the soil layer (base acceleration up to free field motion). The sand has a high relative density (D = 90 %) an angle of internal friction of $\varphi = 45°$, $d_{60} = 0{,}2$ mm, $\rho = 1{,}65$ kN s^2/m^4, $U = 1{,}68$, $v_S = 134$ m/s, $G = 30.000$ kN/m² and $\nu = 0{,}33$. Test parameters are frequency, amplitude and duration of excitation. For more detailed informations about test field and test procedure see (Ref. 6, 7, 8).

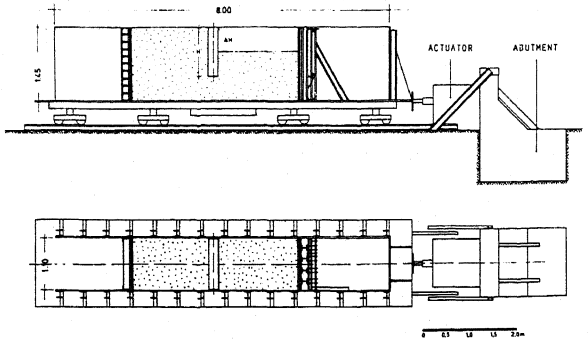

Fig. 1: Test equipment

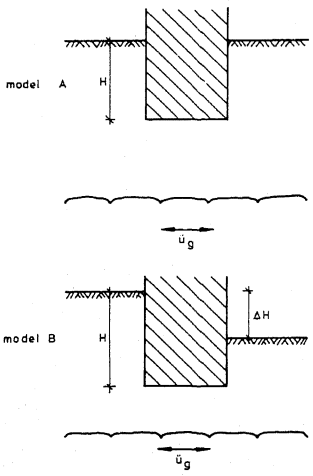

Fig. 2: Investigated models

NUMERICAL INVESTIGATIONS

The numerical model is based on the FE-Method. A computer program system "DYBAST" (Ref. 9) was developed at the TU Berlin for calculation of dynamic behavior of two - and three dimensional soil structure problems. This system uses transmitting boundaries for simulation of energy radiation. Fig. 3 shows a typical FE-model including three typs of elements: beams elements for the structure, elastic plane strain elements for soil and semifinite layer elements for transmitting boundaries (Ref. 10, 11).

All calculations assume linear elastic behavior of the soil and a nearly rigid structure. The dynamic load is defined as the base motion at the bottom (rock). Calculations are in the frequency domain.

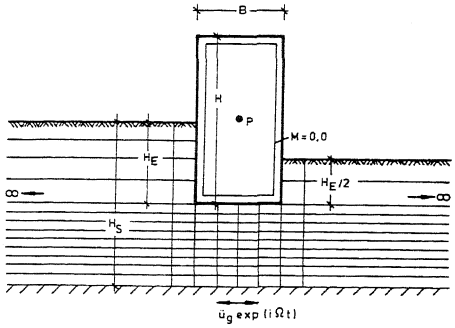

Fig. 3: Finite Element model

RESULTS

The response of the FE-model (see fig. 3) was investigated for different embedment ratios of the structure and several frequencies. Fig. 4 shows for example plots of displacements versus time (model A: $H_E/H_S = 0{,}5$) for the frequency $\Omega = 32$ ($\Omega = \frac{2\pi}{T}$). The experimental response behavior of model B is shown in fig. 5. Displacement amplitude is of oscillating characteristic analogous to the harmonic excitation ($f = 6$ Hz, $\ddot{u}_g = 1{,}5$ m/sec^2) with a slight decrease over time. The significant "stop" during change of movement from direction A to B follows the peak acceleration value of the shaking table. At $t = 0{,}2$ sec the displacement amplitude has a value ob $u_b = 2{,}46$ mm. Also the course of horizontal stresses on both sides of the model structure is of oscillatory nature. During movement of the model towards the backfill (side A) pressure developments of both pressure meters in the interfaces are similar except for a slight retarded course of P 2. An analysis at $t = 0{,}2$ sec gives a retarded increase of both pressure meters during the structure moves outwards until its vertical position of the model structure is reached. With further movement in this direction (to side B) the increase of pressure becomes stronger especially for P 1. With time this increase becomes smaller for P 1 and slightly stronger for P 2. This increasing pressure amplitude follows the outward movement of the structure and this leads to a decrease of dynamic earth pressure at side A. Measured dynamic earth pressure consists of three significant parts: 1) static initial stress e; 2) elastic dynamic part $\tilde{e}^s$ and 3) plastic dynamic part Δe^s. Distribution of the two

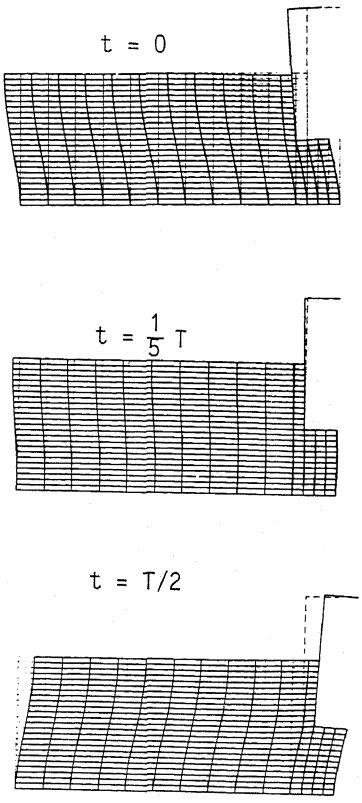

Fig. 4: Model A-response over time

dynamic parts resulting from experimental investigations in the interfaces between model structure and surrounding soil are presented in fig. 6 as well as numerically calculated horizontal stresses for the elastic part $\tilde{e}^S$ (Ref. 9). The aim of the analysis is the verification of the stationary elastic part $\tilde{e}^S$. The Finite Element model used represents the test data and parameters. In the corners of the model base a partly plastic state of soil is regarded as well as a reduced base friction. This nonlinear problem was solved by a process of linear iterations in which shear-modulus was updated succesive to the corresponding nonlinear stress - strain relation. Though the characteristic of the pressure distribution are verified quite well the values itself show a difference factor of 2,0 except near the base. The smaller experimental stress $\tilde{e}^S$ of model A (in comparison with those of model B) are verified by an analogous FE-model with a homogeneous soil layer. It should be outlined, that the plastic part of dynamic earth pressure (Δe^S) for model A is approximatly zero. This indicates a nearly elastic behavior of the surrounding soil for excitation levels applied. Fig. 7a shows the horizontal transfer function u_R (relative to the base) for point P (center point) of model A. Parameter is the embedment ratio of the rigid structure. Dimensionless frequency parameter is the ratio of layer depth H_S to the wave number $k = \frac{v_S}{\Omega}$. Putting the resonance frequency of the layer ωj in the relation to $H_O = \frac{H_S \cdot \Omega}{v_S}$ with v_S = shear wave velocity, one get the dimensionless resonance locations

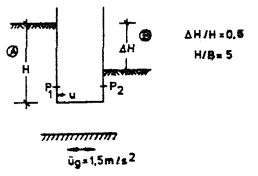

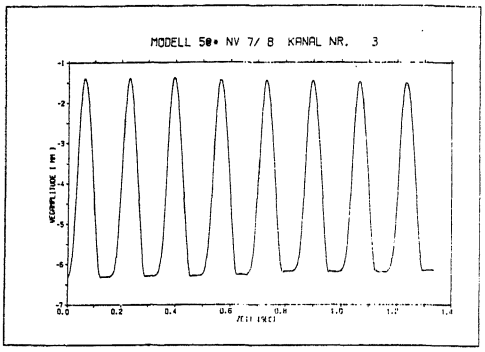

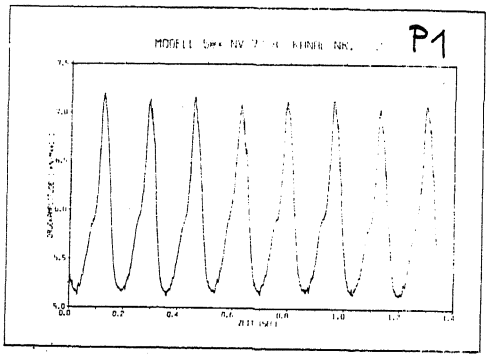

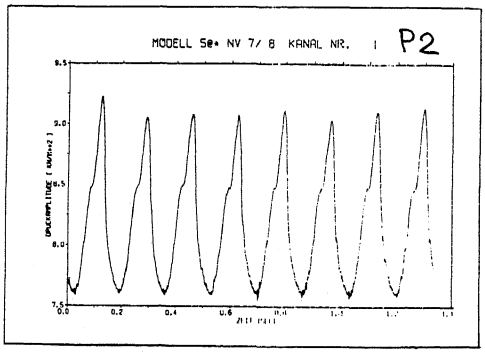

Fig. 5: Model B - displacement and pressure developments

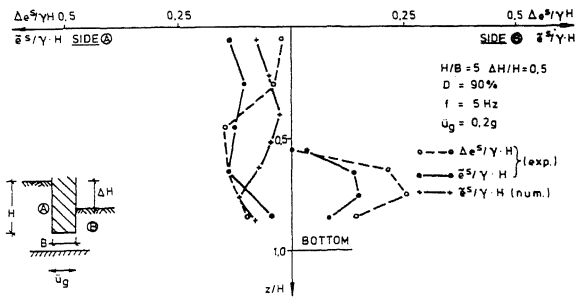

a) model B

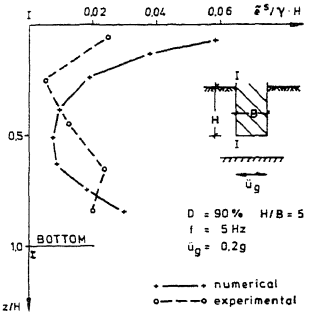

b) model A

Fig. 6: Comparison of horizontal stresses (dynamic part)

$H_{oj} = \frac{\pi}{2} j$ (H_{01} = 1,57; H_02 = 4,71; H_{03} = 7,85)

Internal damping ratio β is chosen to 5 percent. The depth of embedment has a strong influence on the resonance development. The first location of resonance at H_{01} = 1,75 shows an excessive singularity while the resonant amplitudes at H_{02} and H_{03} are strongly damped. The second location of resonance can still be recognized for the ratios H_E/H_S = 0,25 and 0,50. The excessive amplitude-course at H_{01} for all embedment ratios shows that the damping effect due to loss of energy over time appears for higher H_o-values only. It follows that below the first eigenfrequency no geometric energy absorbing occurs. A study of an equivalent damping matrix for the transmitting boundaries shows that the values of the damping matrices are nearly zero. Hence there is no significant interaction between structure and soil for the investigated ratios below H_{01}. For higher H_o-values influence of interaction increases as well as geometrical damping. This follow clearly from fig. 7.

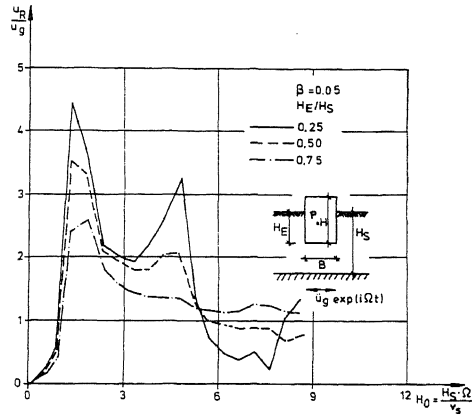

a) model A

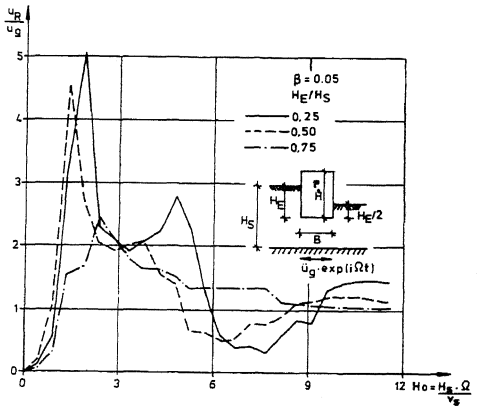

b) model B

Fig. 7: Amplitude transfer functions of horizontal displacement u_R^P (massless structure)

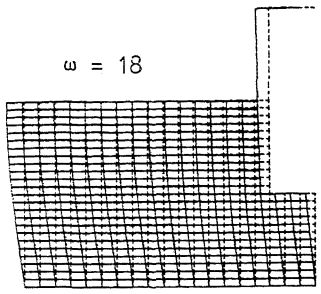

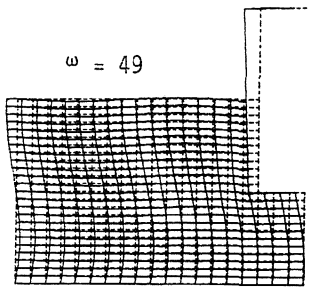

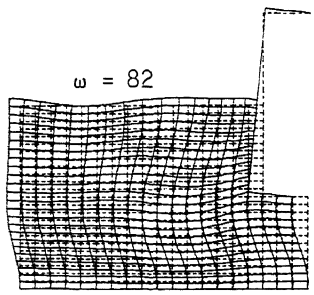

Fig. 8: Model A - real parts of displacement fields

Fig. 7b shows the transfer-function for model B with similar characteristics like for model A. The locations of resonance change due to asymmetric embedment. With increasing ration H_E/H_S the resonance locations of different layer depths affect each other. For side A this location his at $H_{oj} = \frac{\pi}{2} j$ while for side B it's at $H^*_{oj} = H_{oj} \frac{1}{1-1/2H_E/H_S}$. Hence follows for the ratio $H_E/H_S = 0{,}75$ the first resonance location of the right layer at $H^*_{01} = 2{,}5$. For this case there is a coupled vibration of both layers. This follows from fig 7b where the undisturbed resonance locations of the left and right layer lie in the range of $H_0 = 1{,}0$ ./. 3,0. For the ratio $H_E/H_S = 0{,}25$ there is no influence on the resonance locations for different embedments on both sides of the structure. Hence the locations are equal to model A. Fig. 8 presents the real parts of the displacement fields for the first, second and third eigenfrequency of the soil layer for model A. This correspond with the discussed locations of resonance in fig. 7. For frequency $\omega = 18$ the displacement field is approximately identical to the free field motion, as the structure has nearly no influence on response. For $\omega = 49$ and $\omega = 82$ interaction effects are significant regarding the smaler wave lengths of the vertical propagating shear waves. Fig. 9 represents the kinematic interaction for different embedment ratios for both models. The real part of $\frac{u_R}{u_g}$ is indicated as f_1 and the imaginary part as f_2. All figures show the dominant influence of the first layer resonance frequency. This means that in the mathematical model "kinematical interaction" is fairly good represented by the free field model (see Ref. 12). As outlined kinematic interaction becomes more importend for higher frequencies and increasing embedment ratio. For this reason it's more difficult to formulate an approximation of the complex transfer functions in the higher frequency range.

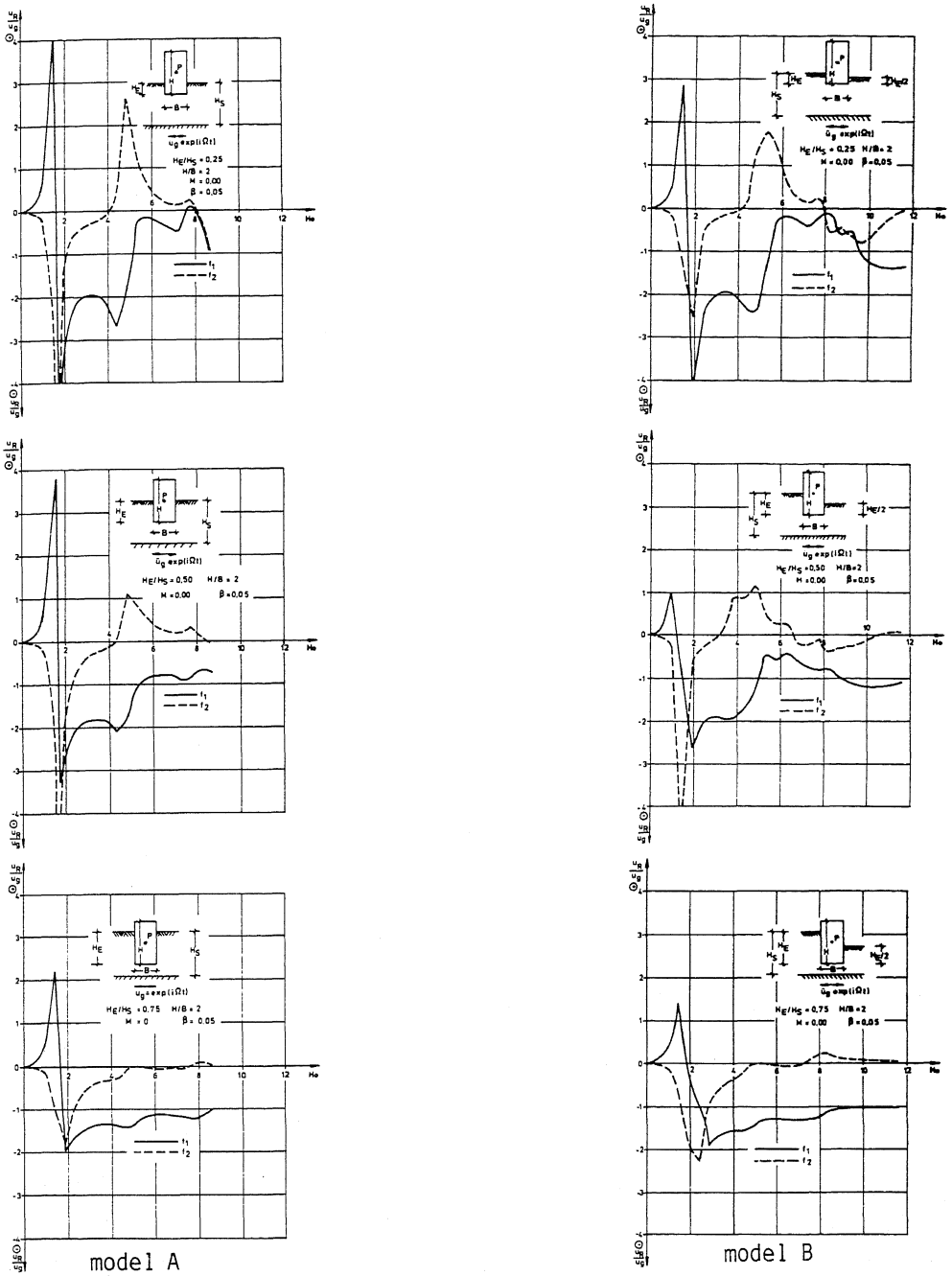

Fig. 9: Complex transfer functions (f_1+if_2) of the horizontal displacement

REFERENCES

(1) MONONOBE, H. (1925): "Design of a Seismic Gravity Wall", Journ.Soc.Civil Engrg.3

OKABE, S. (1924): "General Theorie of Earth Pressure and Seismic Stability of Retaining Wall and Dam", Journ.Soc. Civil. Engrg.4

(2) SEED, B. and WHITMAN, R.V. (1970): "Design of Earth Retaining Structures for Dynamic Loads", Spec.Conf. on Lateral Stresses in the Ground and Design of Earth Retaining Structures, ASCE, S. 103-147

(3) NAZARIAN, H.N. and HANDJIAN, A.H. (1979): "Earthquake Induced Lateral Soil Pressures on Structures", Joun.of the Geotechnik, Engrg.Div., ASCE

(4) WHITMAN, R.V. (1979): "Dynamic Behavior of Soils and its Application to Civil Engineering Projects", Proc. 6th Panamerican Conf. on SMFE, Lima, Peru

(5) KAUSEL, E., LUCHS, A.S., EDGERS, L., SWIGER, W.F. and CHRISTIAN J.T. (1979): "Seismically Induced Sliding of Massive Structures", Journ. of the Geotech. Engrg. Div., GT 12, ASCE

(6) SAVIDIS, S.A., KLAPPERICH, H., SARFELD, W. and SCHUPPE, R. (1982): "Experimental and Numerical Investigations of the Dynamic Earth Pressure", 7th ECEE, Athen

(7) KLAPPERICH, H. (1983): "Untersuchungen zum dynamischen Erddruck" Veröff. des Grundbauinstitutes der TU Berlin, Heft 14

(8) SAVIDIS, S.A. and KLAPPERICH, H. (1983): "Test Area for Dynamic Investigations", Veröff. des Grundbauinstitutes der TU Berlin, Heft 13

(9) SARFELD, W. (1981): "DYBAST" program for dynamic calculations of soil-structures by FEM, TU Berlin

(10) WAAS, G. (1972): "Linear Two-Dimensional Analysis of Soil Dynamic Problems in Semi-Infinite Layered Media", Univer of California, Berkeley

(11) KAUSEL, E. and ROESSET, J.M. (1975): "Dynamic Stiffness of Circular Foundations", Journ. of the Engrg. Mech.Div., ASCE, Vol. 101, No. EM 6

(12) KAUSEL, E. and ROESSET, J.M. (1974): "Soil-Structure-Interaction Problems for Nuclear Containment Structures", ASCE Power Div. Spec.Conf., Denver